

Defects in CTP:PHOSPHORYLETHANOLAMINE CYTIDYLYLTRANSFERASE Affect Embryonic and Postembryonic Development in *Arabidopsis*^W

Junya Mizoi,^a Masanobu Nakamura,^a and Ikuo Nishida^{b,1}

^aDepartment of Biological Sciences, Graduate School of Science, University of Tokyo, Bunkyo-ku, Tokyo 113-0033, Japan

^bDepartment of Life Science, Graduate School of Science and Engineering, Saitama University, Sakura-ku, Saitama City, Saitama 338-8570, Japan

A TILLING strategy (for targeting-induced local-scale lesions in genomes) was used in *Arabidopsis thaliana* to isolate mutants of a gene encoding CTP:PHOSPHORYLETHANOLAMINE CYTIDYLYLTRANSFERASE (PECT; EC 2.7.7.14), a rate-limiting enzyme in phosphatidylethanolamine biosynthesis. A null mutation, *pect1-6*, caused embryo abortion before the octant stage. However, reciprocal crosses revealed that *pect1-6* caused no significant gametophytic defect. In *pect1-4*, PECT activity was decreased by 74%. Growth was generally normal in these mutants, despite delays in embryo maturation and reduced fertility. At low temperatures, however, homozygotic *pect1-4* plants displayed dwarfism. PECT activity was decreased by 47% in heterozygotic *pect1-6* plants and by 80% in *pect1-4/pect1-6* F1 plants, which also displayed a small but significant decrease of phosphatidylethanolamine and a reciprocal increase in phosphatidylcholine. These lipid changes were fully reversed by wild-type *PECT1* expression. *pect1-4/pect1-6* F1 plants displayed severe dwarfism, tissue abnormalities, and low fertility, which was attributable in part to inhibition of anther, embryo, and ovule development, as was the reduced fertility of *pect1-4* seedlings. *PECT1* cDNA expression under the control of an inducible promoter partially rectified the mutant phenotypes observed in *pect1-4/pect1-6* F1 seedlings, indicating that malfunctions in different tissues have a synergistic effect on the mutant phenotypes.

INTRODUCTION

Phosphatidylethanolamine (PE) is a nonbilayer lipid in the cell membrane of bacteria, yeast, and higher eukaryotes that plays important roles in cell division and protein secretion. PE is required for the organization of FtsZ division rings in *Escherichia coli* (Mileykovskaya et al., 1998) and for the disassembly of a contractile ring in Chinese hamster (*Cricetulus griseus*) ovary cells (Emoto and Umeda, 2000). In *E. coli*, PE is also required for the activity of LacY lactose permease, a membrane-bound enzyme (Bogdanov and Dowhan, 1995). Yeast (*Saccharomyces cerevisiae*) cells require PE for the maturation of the glycosylphosphatidylinositol-anchored protein Gas1p (Birner et al., 2001) and for the targeting of proton motive force transporters to the plasma membrane (Robl et al., 2001; Opekarová et al., 2002). Inhibition of PE synthesis causes developmental defects in the nervous system of *Drosophila melanogaster* (Pavlidis et al., 1994) and embryonic lethality in mice (*Mus musculus*) as a result of abnormal mitochondrial development (Steenbergen et al., 2005). However, the physiological consequences of inhibiting PE biosynthesis in plants require investigation by molecular genetics.

PE is the major phospholipid in all plant membranes except plastids (Douce et al., 1973). It is synthesized via three pathways: the cytidyldiphosphate-ethanolamine (CDP-Etn) pathway, the phosphatidylserine (PS) decarboxylation pathway, and the base-exchange pathway (Kinney, 1993). The CDP-Etn pathway involves three sequential reactions catalyzed by ethanolamine kinase (EC 2.7.1.82), CTP:phosphorylethanolamine cytidylyltransferase (PECT; EC 2.7.7.14), and CDP-ethanolamine:diacylglycerol ethanolaminephosphotransferase (EC 2.7.8.1), respectively. PECT is considered the rate-limiting enzyme in the CDP-Etn pathway (Tang and Moore, 1997). The genome of *Arabidopsis thaliana* contains a single PECT gene (*PECT1*; At2g38670) (Arabidopsis Genome Initiative, 2000). cDNA from this gene has been isolated, and the enzyme activity of a recombinant gene product has been measured (Mizoi et al., 2003). The second pathway, PS decarboxylation, is catalyzed by PS decarboxylase (EC 4.1.1.65). The tomato (*Solanum lycopersicum*) gene encoding a mitochondrial PS decarboxylase has been isolated and characterized (Rontein et al., 2003). However, three putative *Arabidopsis* genes for PS decarboxylase, *PSD1*, *PSD2*, and *PSD3*, have yet to be fully characterized (Rontein et al., 2003). The third pathway for PE synthesis, base exchange, is catalyzed by PS synthase. Two isoforms of PS synthase are present in mammalian cells. This enzyme exchanges the Ser residue of PS for either Etn or choline to synthesize PE or phosphatidylcholine (PC), respectively (Kuge et al., 1986). Although there is one putative *Arabidopsis* PS synthase gene (*PSS1*; At1g15110) (Arabidopsis Genome Initiative, 2000), the enzyme activity of its gene product has yet to be described. Isolation of gene mutants of key PE biosynthetic

¹ To whom correspondence should be addressed. E-mail nishida@molbiol.saitama-u.ac.jp; fax 81-48-858-3384.

The author responsible for distribution of materials integral to the findings presented in this article in accordance with the policy described in the Instructions for Authors (www.plantcell.org) is: Ikuo Nishida (nishida@molbiol.saitama-u.ac.jp).

^W Online version contains Web-only data.

www.plantcell.org/cgi/doi/10.1105/tpc.106.040840

enzymes is essential for evaluating the importance of PE in plants.

A number of mutants with altered fatty acid composition have been isolated with forward genetics (Somerville and Browse, 1991; Wallis and Browse, 2002), whereas reverse genetics has been useful to isolate and characterize mutants with altered polar lipid metabolism (Hagio et al., 2002; Yu et al., 2002, 2004; Kelly et al., 2003; Zheng et al., 2003; Kim and Huang, 2004; Kim et al., 2005). T-DNA-tagged lines for *Arabidopsis* genes encoding plastid-targeted lysophosphatidic acid acyltransferase (LPAAT; *LPAT1/ATS2*) (Kim and Huang, 2004; Yu et al., 2004), an endoplasmic reticulum-targeted LPAAT (*LPAT2*) (Kim et al., 2005), and plastid-targeted phosphatidylglycerophosphate synthase (*PGP1*) (Hagio et al., 2002; Babiychuk et al., 2003) are all lethal, impeding further investigation of these mutants. Isolating a series of ethyl methanesulfonate-mediated point mutants for genes encoding key enzymes is critical for studying the physiological consequences of altered lipid metabolism. The TILLING strategy (for targeting-induced local-scale lesions in genomes) screens for a dozen mutant alleles within a specific genomic region of interest (Till et al., 2003), thus allowing the identification of mutants with different degrees of severity.

With the aid of TILLING, we have identified 11 *pect1* alleles with mutations within a 1.0-kb genomic region of *PECT1*, and we report the phenotypes of the null mutant *pect1-6*, the mild mutant allele *pect1-4*, and the transheterozygotic mutant *pect1-4/pect1-6*. The results show that the CDP-Etn pathway is essential for early embryonic development in *Arabidopsis*. Decreasing PECT activity causes pleiotropic abnormalities in embryonic and postembryonic development of this plant. We also show that fluorescently tagged PECT1 colocalizes with mitochondria, suggesting mitochondrial involvement in PE biosynthesis.

RESULTS

Identification and Characterization of *pect1* Alleles That Cause Reduced PECT Activity

TILLING was used to screen for *pect1* alleles carrying point mutations within the region encoding the first of two putative catalytic domains of PECT1 (i.e., nucleotides 121 to 1091) (Figure 1A). Eleven mutant alleles were identified (Table 1); of these, *pect1-2*, *pect1-3*, *pect1-4*, *pect1-6*, and *pect1-9* were selected for further analysis because each had a single base substitution, C287T, C301T, C465T, and C883T, resulting in the amino acid substitutions A96V, P101S, P126S, and S232L, respectively. The *pect1-6* allele carries a G649A substitution at the splicing donor site of the second intron. Three unusual *pect1-6* transcripts were identified by RT-PCR, but none is likely to produce catalytically active proteins (see the legend of Supplemental Figure 1 online). A D64N substitution within the first catalytic domain was predicted for the *pect1-1* mutant, which we attempted to characterize but failed to isolate from the corresponding seed stock. *pect1-7*, *pect1-8*, *pect1-10*, and *pect1-11* alleles also were not characterized, but we predicted that these mutations alter amino acid residues that are not conserved among known PECT proteins. In rosette homogenates from homozygous mutants

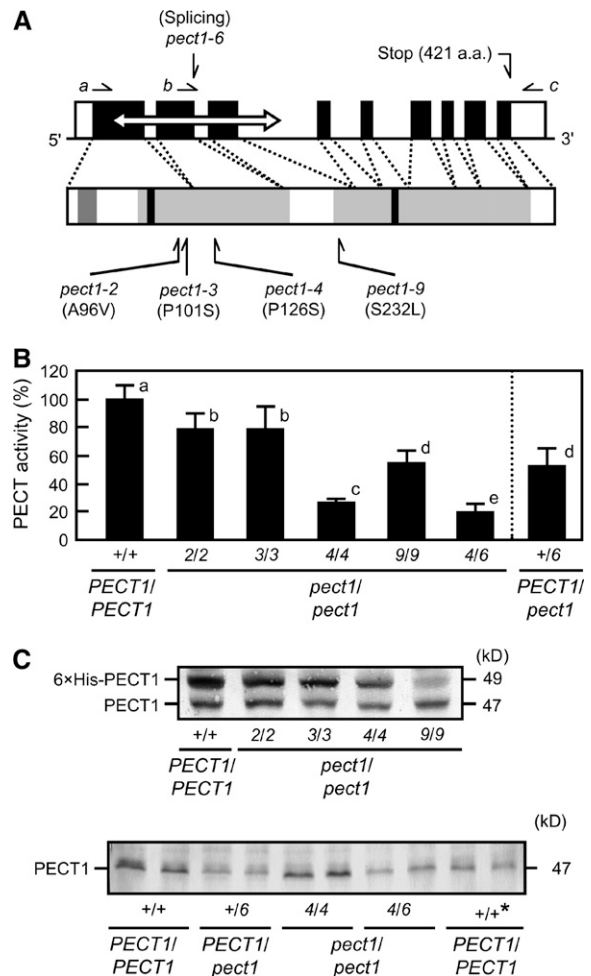


Figure 1. Isolation and Characterization of *pect1* Allelic Mutants.

(A) Scheme of the *PECT1* gene and the PECT1 protein. Top, the gene structure includes 5' and 3' untranslated regions (open boxes), coding exons (closed boxes), and introns (lines between exons). The total length of the coding sequence of *PECT1* from the start codon to the stop codon is 2701 bp. The open arrow indicates the region used for our TILLING search. Each arrow indicates an isolated *pect1* mutation. Bottom, the protein structure includes a putative transmembrane region (dark gray box), the HXGH core sequences (black boxes), and conserved catalytic domains (light gray boxes). a.a., amino acids.

(B) PECT activity in homogenates of mutant rosette leaves. PECT activities per protein base are presented as percentages relative to wild-type rosette leaves. The data shown are averages of more than seven assays from more than two independent experiments. Error bars indicate sd. Data with the same letter are not significantly different at $P < 0.01$.

(C) Immunoblot analysis of PECT1. Top, each lane was loaded with 27 μ g of protein from rosette homogenate. Different amounts of recombinant 6xHis-PECT1 were used as linearity controls for densitometry. Bottom, each lane contained 65 μ g of protein from rosette homogenate, except the last two lanes (indicated by the asterisk), which were loaded with 32.5 μ g of protein.

Table 1. Summary of *pect1* Alleles

| Allele | Accession Number ^a | Mutant Isolation ^b | Base Alteration | Amino Acid Alteration | Mutation Type | Amino Acid Residues in the Corresponding Position | | | |
|-----------------|-------------------------------|-------------------------------|-----------------|-----------------------|---------------|---|--------------------------|----------------------|--------------------|
| | | | | | | Angiosperms ^c | Green Algae ^d | Mammals ^e | Yeast ^f |
| <i>pect1-1</i> | 139F6 | No | G190A | D64N | Missense | D | D | D | D |
| <i>pect1-2</i> | 184A1 | Yes | C287T | A96V | Missense | A | R | K | H |
| <i>pect1-3</i> | 142F4 | Yes | C301T | P101S | Missense | P | P | P | P |
| <i>pect1-4</i> | 175A6 | Yes | C465T | P126S | Missense | P | P | P | P |
| <i>pect1-5</i> | 144G6 | – | G509A | E140E | Silent | E/K | K | K | K |
| <i>pect1-6</i> | 139F6.1 | Yes | G649A | Null | Junction | | | | |
| <i>pect1-7</i> | 143G3 | – | G775A | R196K | Missense | R/none ^g | None | None | None |
| <i>pect1-8</i> | 139C2 | – | C862T | S225F | Missense | F/D/none | None | None | None |
| <i>pect1-9</i> | 145A3 | Yes | C883T | S232L | Missense | S | S | S | None |
| <i>pect1-10</i> | 176F8 | – | C894T | P236S | Missense | P | P | Q | None |
| <i>pect1-11</i> | 139A2 | – | C895T | P236L | Missense | P | P | Q | None |

^a Accession numbers in the polymorphism database at The Arabidopsis Information Resource. Data are registered in the designation of atpect1_139F6 in the database.

^b Yes, successful; no, unsuccessful; –, not attempted.

^c *Hordeum vulgare* (AY198340), *Oryza sativa* (AK099943 and AK068868), and *Solanum lycopersicum* (BT013823).

^d *Chlamydomonas reinhardtii* (AY234844).

^e *Homo sapiens* (D84307) and *Rattus norvegicus* (AF080568).

^f *Saccharomyces cerevisiae* (D50644).

^g None, no corresponding amino acid residue was found in the alignment.

backcrossed at least once, *pect1-2*, *pect1-3*, *pect1-4*, and *pect1-9* retained 78.6, 78.8, 25.9, and 54.3% of PECT activity per milligram of protein in the homogenates, respectively, compared with wild-type plants (Figure 1B). In rosette leaf extracts of these four mutants, an anti-PECT1 antiserum recognized a single protein band, the size and intensity of which were similar to those of wild-type PECT1 (Figure 1C). These results suggest that each of these alleles produces a mutant protein with lower specific activity than wild-type PECT1.

The *pect1-6* allele was not maintained in homozygous plants. Heterozygous *PECT1/pect1-6* plants exhibited ~50% of the PECT activity observed in rosette homogenates from wild-type plants (Figure 1B). Immunoblot analysis revealed a single band in *PECT1/pect1-6* homogenates, the same size and half the intensity of wild-type PECT1, indicating that there is a gene dosage effect (Figure 1C). Thus, PECT activity in *PECT1/pect1-6* plants can be ascribed to wild-type *PECT1*. These results suggest that *pect1-6* is a null mutant allele of the *PECT1* locus. Because *pect1-4* and *pect1-6* mutants exhibited significant defects in PECT activity, we focused on these mutants, which were backcrossed more than three times for further analyses.

The Recessive Null Allele *pect1-6* Causes Seed Abortion

PECT1/pect1-6 plants were indistinguishable from wild-type plants when grown at 23°C under continuous illumination at a photon flux density of 75 $\mu\text{mol}\cdot\text{m}^{-2}\cdot\text{s}^{-1}$. However, developing siliques of self-fertilized *PECT1/pect1-6* plants contained a significant number of seeds ($n = 525$) with an aborted appearance (Figure 2B). These seeds were segregated from normal seeds ($n = 1603$) at a ratio of 1:3 ($P > 0.5$), suggesting that *pect1-6* is a single recessive nuclear allele that causes seed abortion in

Arabidopsis. Cosegregation experiments with a 6.5-kb *PECT1* gene fragment (designated *transPECT1*) under the control of a full-length *PECT1* promoter of 0.5 kb (*PROPECT1*) verified that *pect1-6* causes seed abortion (Figure 2C; see Supplemental Table 1 online).

The *pect1-6* Allele Causes Embryonic Lethality by the Octant Stage

To clarify the mechanism of seed abortion in *pect1-6* seeds, developing siliques of self-fertilized *PECT1/pect1-6* plants were cleared in a trichloroacetaldehyde solution for observation of the internal structure with a differential interference contrast microscope equipped with Nomarski optics. In siliques of *PECT1/pect1-6* plants, only seeds that carried *pect1-6* embryos were expected to have abnormal structures. The proportion of abnormal seeds within these siliques supported this hypothesis (see Supplemental Tables 2 and 3 online). Two days after flowering, abnormal *pect1-6* embryos had one to four cells and were surrounded by endosperms with enlarged nuclei (Figure 2D, abnormal), whereas normal embryos were at the single-cell to early-globular stages (Figure 2D, normal). However, 4 d after flowering, when normal embryos reached the transition or heart stage (Figure 2E, normal), most *pect1-6* embryos had decayed so much that it was impossible to determine their embryonic stage. The remaining *pect1-6* embryos displayed an aborted appearance: one- or two-cell embryos without nuclei (Figure 2E, abnormal, left) or eight-cell embryos without nuclei (Figure 2E, abnormal, right). These results suggest that homozygotic *pect1-6* mutant embryos do not develop beyond the octant stage, resulting in seed abortion.

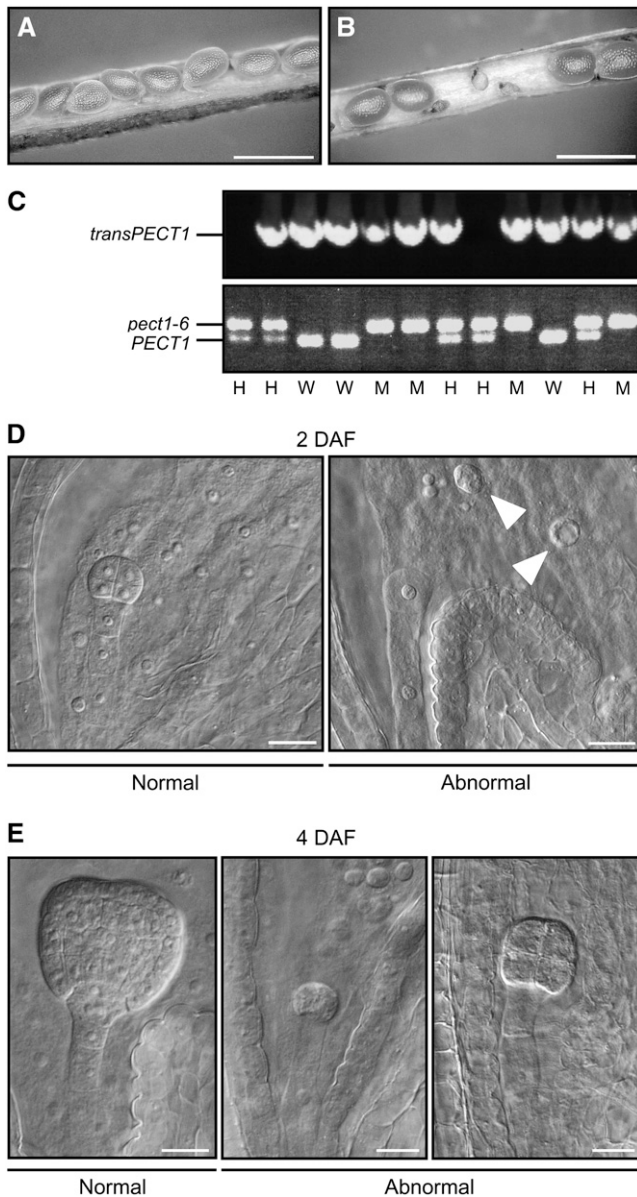


Figure 2. The *pect1-6* Allele Causes Seed Abortion as a Result of Abnormal Embryo Development.

(A) An opened silique from a wild-type plant.
 (B) An opened silique from a *PECT1/pect1-6* plant.
 (C) Genotyping of F2 seedlings from a *PECT1/pect1-6 transPECT1/-* F1 plant. Top, detection of *transPECT1* by PCR. Bottom, detection of *PECT1* and *pect1-6* by derived cleaved-amplified polymorphic sequence (dCAPS) analysis. Results are shown for the F2 seedlings of a *PECT1/pect1-6 transPECT1/-* plant line with a 7% seed abortion rate (see the legend of Supplemental Table 1 online). No homozygous *pect1-6* mutant line was identified that did not carry *transPECT1*, indicating that *pect1-6* causes seed abortion. Wild type (W), heterozygous (H), and mutant (M) represent the F2 seedling genotypes *PECT1/PECT1*, *PECT1/pect1-6*, and *pect1-6/pect1-6*, respectively.
 (D) and (E) Differential interference contrast images of embryos in seeds of self-fertilized *PECT1/pect1-6* plants at 2 d (D) and 4 d (E) after flowering.

No significant gametophytic defect was observed when *PECT1/pect1-6* plants were reciprocally crossed with wild-type plants (see Supplemental Table 4 online), indicating that the *pect1-6* allele does not impair the development of male and female gametophytes or their fertilization processes in *PECT1/pect1-6* plants. However, the number of seeds tested ($n \leq 92$) was not sufficient to exclude the possibility that gametophytic defects might be significant if larger numbers of seeds were examined.

The Homozygous *pect1-4* Allele Permits Almost Normal Growth at Room Temperature but Causes Dwarfism at Low Temperature

When grown at 23°C for 18 d under continuous illumination at a photon flux density of $75 \mu\text{mol}\cdot\text{m}^{-2}\cdot\text{s}^{-1}$, *pect1-4* plants were indistinguishable from or slightly smaller than wild-type plants. However, *pect1-4* plants showed dwarfism when grown at 8°C, either under a day/night light regime with an 8-h photoperiod at a photon flux density of $75 \mu\text{mol}\cdot\text{m}^{-2}\cdot\text{s}^{-1}$ as above (Figure 3A) or under continuous light at a photon flux density of $30 \mu\text{mol}\cdot\text{m}^{-2}\cdot\text{s}^{-1}$ (Figure 3B). In plants grown further under the day/night light regime, the number of rosette leaves in *pect1-4* plants did not differ from that in wild-type plants, and dwarfism at low temperature was suppressed by cosegregation with the *transPECT1* gene fragment (Figure 3A), indicating that homozygous *pect1-4* permits rosette leaf formation but limits growth at low temperature. In addition, both cotyledons and mature leaves of *pect1-4* plants senesced earlier than those of wild-type plants. The mutant phenotypes observed at low temperatures will be investigated further in future studies.

The fertility of plants grown at ambient temperature was partially reduced as a result of the development of short or immature anther filaments (Figure 3C). However, as described below, when male organs were infertile, accompanying stigmas appeared to increase the proportion of embryo sac abortion, caused by a sporophytic defect.

Homozygous *pect1-4* Delays Embryo Maturation

pect1-4 seeds looked pale green and were smaller than *PECT1* and *PECT1/pect1-4* seeds when borne in the siliques of *PECT1/pect1-4* plants (Figure 3D). No *transPECT1* was detected in embryos from pale green seeds of *pect1-4/pect1-4 transPECT1/-* plants (data not shown), indicating that *pect1-4* causes the pale-green-seed phenotype. Embryo populations in the developing seeds of self-fertilized *PECT1/pect1-4* plants varied

(D) A typical octant-stage embryo from a normal seed (left; normal), and a typical mutant embryo from a mutant seed (right; abnormal). Average diameters of the endosperm nuclei were $3.4 \pm 0.6 \mu\text{m}$ ($n = 59$) and $7.8 \pm 2.2 \mu\text{m}$ ($n = 34$) for wild-type and *pect1-6* endosperms, respectively. Arrowheads indicate enlarged nuclei. The size of the mutant endosperm nuclei did not increase significantly until embryo abortion.

(E) A typical transition-stage embryo in a normal seed (left; normal), and typical mutant embryos in aborted seeds (middle and right; abnormal). Bars = 1 mm for (A) and (B) and 20 μm for (D) and (E).

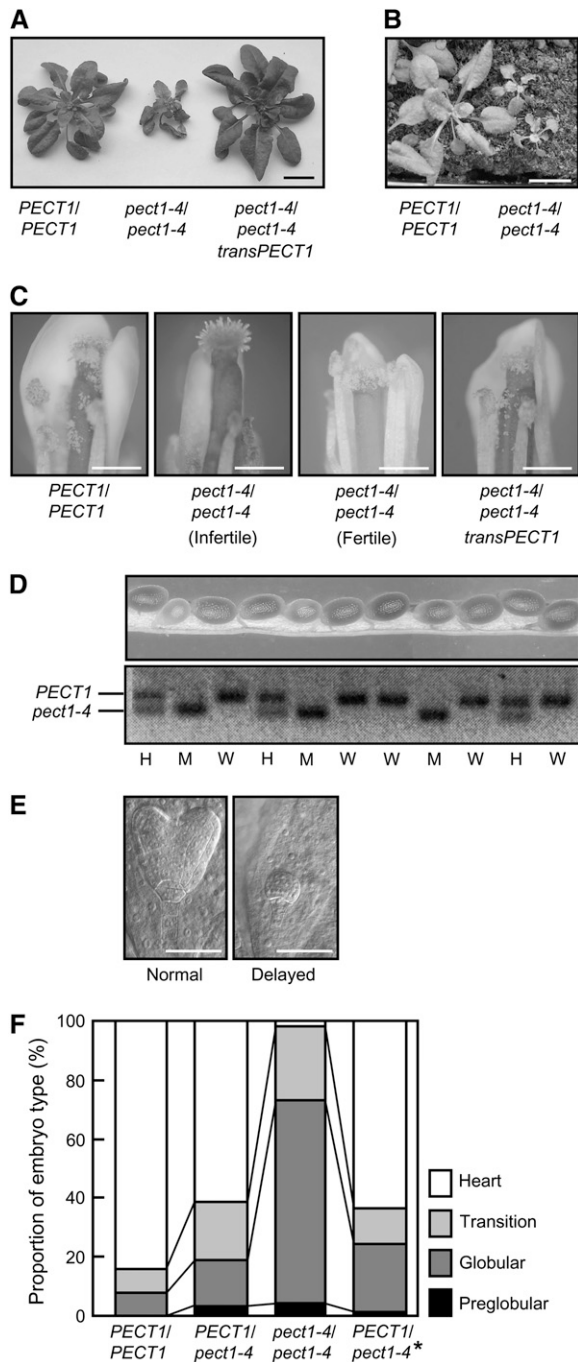


Figure 3. Mutant Phenotypes of *pect1-4* Plants.

(A) and (B) *pect1-4/pect1-4* plants exhibit dwarfism at low temperature. (A) Wild-type (left), homozygous *pect1-4* (middle), and *transPECT1*-transformed homozygous *pect1-4* plants (right) were grown at 23°C for 14 d under continuous illumination at a photon flux density of 75 $\mu\text{mol}\cdot\text{m}^{-2}\cdot\text{s}^{-1}$ and then grown for an additional 42 d at 8°C under a day/night light regime with an 8-h photoperiod at a photon flux density of 75 $\mu\text{mol}\cdot\text{m}^{-2}\cdot\text{s}^{-1}$.

(B) Wild-type and *pect1-4/pect1-4* plants were grown at 23°C for 14 d and then grown for another 30 d at 8°C under continuous light at a photon flux density of 30 $\mu\text{mol}\cdot\text{m}^{-2}\cdot\text{s}^{-1}$.

widely at 4 d after flowering (see Supplemental Table 5 online). Examination of the proportion of embryos at each stage suggested that most normal (*PECT1* and *PECT1/pect1-4*) embryos reached the heart stage, whereas most delayed (*pect1-4*) embryos only reached the early-globular stage (Figure 3E). Four days after manual pollination with their own pollen, embryo populations within the seeds of *PECT1/PECT1* ($n = 7$), *PECT1/pect1-4* ($n = 10$), and *pect1-4/pect1-4* ($n = 4$; all fertile) descendants of a *PECT1/pect1-4* plant were scored with the use of a microscope (see Supplemental Table 6 online). As summarized in Figure 3F, the embryo populations within seeds of fertile *pect1-4/pect1-4* plants had delayed maturation profiles compared with the embryos within the seeds of *PECT1/PECT1* plants. Embryo populations within the seeds of *PECT1/pect1-4* plants resembled our predicted profile (*PECT1/pect1-4** in Figure 3F), which assumed a 3:1 segregation for normal (*PECT1/PECT1* and *PECT1/pect1-4*) versus delayed (*pect1-4/pect1-4*) embryo phenotypes. A partial defect in *PECT1/pect1-4* embryos, therefore, is unlikely, supporting the view that only homozygous *pect1-4* delays embryo maturation. Aborted seeds were rarely found in the siliques of self-fertilized *PECT1/pect1-4* plants, suggesting that all delayed embryos reach maturation before seed desiccation.

pect1-4/pect1-6 F1 Plants Exhibit Pleiotropic Abnormalities in Both Vegetative and Reproductive Tissues

Cellular PECT activity showed a gene dosage effect (Figures 1B and 1C). Therefore, *PECT1/pect1-4* plants were crossed with *PECT1/pect1-6* plants to generate F1 plants, *pect1-4/pect1-6*, with significantly reduced PECT activity. The resultant transheterozygotic plants were expected to exhibit half the PECT activity of *pect1-4* plants. However, these transheterozygotic plants retained 19.4% of wild-type PECT activity per milligram of

(C) Photographs of flowers opened manually at 1 d after flowering. The genotype and fertility of each flower are shown.

(D) Small-seed phenotype of *pect1-4* seeds. Shown is the middle part of an opened silique from a *PECT1/pect1-4* plant at 6 d after flowering. Seeds are either green with bent-cotyledon-stage embryos or pale green with small green embryos. Genotyping of the depicted embryos revealed that the green-seed embryos are homozygous or heterozygous for *PECT1* ($n = 15$) and the pale-green-seed embryos are homozygous for *pect1-4* ($n = 5$). The genotype of each embryo is indicated below each lane. The letters W, H, and M represent wild-type *PECT1/PECT1*, heterozygous *PECT1/pect1-4* mutants, and homozygous *pect1-4/pect1-4* mutants, respectively.

(E) Differential interference contrast images of embryos in siliques from a *PECT1/pect1-4* plant at 4 d after flowering. Typical images of normal and delayed embryos are shown.

(F) Proportions of different embryo types in seeds from *PECT1/PECT1*, *PECT1/pect1-4*, and *pect1-4/pect1-4* plant siliques at 4 d after manual self-pollination. *PECT1/pect1-4** represents the predicted embryo population in *PECT1/pect1-4* siliques calculated from the embryo populations in *PECT1/PECT1* and *pect1-4/pect1-4* plant siliques, assuming a 3:1 segregation for normal (*PECT1/PECT1* and *PECT1/pect1-4*) versus delayed (*pect1-4/pect1-4*) embryos.

Bars = 1 cm for (A) and (B), 0.5 cm for (C), and 50 μm for (E).

protein in the rosette homogenates, which was equivalent to 74.9% of the PECT activity in *pect1-4* plants (Figure 1B). PECT1 levels in *pect1-4/pect1-6* F1 plants were almost half those of *pect1-4* plants (Figure 1C), suggesting that the *pect1-4* protein may be slightly activated in *pect1-4/pect1-6* F1 plants.

pect1-4/pect1-6 F1 plants showed severe dwarfism compared with age-matched wild-type plants (Figure 4A). Main stem sections of these plants had smaller cell numbers in the cortex and pith and reduced cell length in the pith (Figures 4B and 4C), both of which could explain the dwarfism. As a result of reduced stele volumes, stem radius was also reduced in transheterozygotic plants (Figures 4D and 4E). Reduced numbers of vascular bundles (Figures 4D and 4E) and delayed xylem, phloem, and cambium development (Figures 4F and 4G) were common features in *pect1-4/pect1-6* plant stems and major leaf veins (data not shown) that can result in less efficient nutrient translocation. The secondary walls in xylem and interfascicular fiber cells of mature stems were thinner in transheterozygotes (Figure 4G) than in the wild type (Figure 4F), suggestive of altered cell wall metabolism. Furthermore, the rosette leaves of *pect1-4/pect1-6* F1 plants showed an early-senescence phenotype (Figure 4A, arrows). Cell enlargement and intercellular space development in leaves were inhibited in transheterozygotes (Figure 4I; cf. the wild type in Figure 4H), and the root meristematic zone was shorter in transheterozygotes than in the wild type (Figures 4J and 4K, asterisks). In addition, the walls of columella cells within the root cap of transheterozygotic seedlings were disordered (Figure 4M), in contrast with the regularly aligned cell walls observed in wild-type seedlings (Figure 4L).

Partial Embryo Abortion in *pect1-4/pect1-6* Siliques

Fertility was severely reduced in a subpopulation of transheterozygotic *pect1-4/pect1-6* plants as a result of short anther filaments (Figure 4O), reduced pollen volume (Figure 4O), and/or inhibition of anther maturation (Figure 4P). Self-fertilized *pect1-4/pect1-6* F1 plants developed 40% fewer placentas per silique than wild-type plants (see Supplemental Table 7 online), and a large proportion (~75%) of ovules remained unfertilized in *pect1-4/pect1-6* siliques. Consequently, the number of normal seeds per silique seldom reached 10 (1 of 90 siliques), and 42% of siliques (38 of 90) produced no seed.

pect1-6 seeds, which underwent early death, were expected to occur at a segregation rate of 25% in the offspring of *pect1-4/pect1-6* F1 plants. More than 50% of fertilized seeds were aborted in siliques of *pect1-4/pect1-6* F1 plants (see Supplemental Table 7 online), suggesting that *pect1-4/pect1-6* is partially lethal. Crossing *PECT1/pect1-6* (female) and *pect1-4/pect1-4* (male) plants confirmed this hypothesis (see Supplemental Table 8 online). A significant proportion (~25%; 29 of 117) of *pect1-4/pect1-6* seeds were aborted in the siliques of *PECT1/pect1-6* plants.

Homozygotic *pect1-4* and *pect1-4/pect1-6* Significantly Increase the Proportion of Embryo Sac Abortion

As described above, fertility was reduced in both *pect1-4* and *pect1-4/pect1-6* F1 plants as a result of partial inhibition of male

organ development in these plants (Figures 3C, 4O, and 4P). To determine whether stigmas were fertile when accompanying male organ development was severely inhibited, reciprocal crosses were performed and the number of different ovules and embryos was scored with the use of a microscope (see Supplemental Table 9 online). In populations of *pect1-4/pect1-6* flowers whose anthers appeared fertile, approximately one-third of the ovules from crosses between *pect1-4/pect1-6* stigmas and wild-type pollen (cross 8 in Supplemental Table 9 online) developed abnormal embryo sacs (Figures 4R and 4S; cf. the normal embryo sacs in wild-type plants in Figure 4Q). Crossing stigmas from *pect1-4* flowers whose anthers appeared infertile with wild-type pollen also produced ovules with abnormal embryo sacs (~50%; cross 6 in Supplemental Table 9 online), and this proportion was reduced when *pect1-4* flowers whose anthers appeared fertile were crossed with wild-type pollen (~10%; cross 5 in Supplemental Table 9 online). By contrast, abnormal ovules were greatly reduced when *PECT1/pect1-6* stigmas (2.7%; cross 3 in Supplemental Table 9 online) or wild-type stigmas (<2.6%; cross 4 in Supplemental Table 9 online) were crossed with wild-type pollen. Thus, homozygotic *pect1-4* and *pect1-4/pect1-6* increase the rate of embryo sac abortion, reflecting defects in female gametophyte formation or maturation in a portion of ovules. Emasculated infertile *pect1-4/pect1-4* flowers produced larger proportions of abnormal ovules than emasculated fertile *pect1-4/pect1-4* flowers (see Supplemental Table 10 online). The effect may be an incompletely penetrant sporophytic defect rather than a gametophytic effect.

Tissue Malfunctions Act Synergistically to Enhance Mutant Phenotypes of *pect1-4/pect1-6* F1 Plants

The defects observed in *pect1-4/pect1-6* transheterozygotes were not rescued by exogenous application of CDP-Etn, 1-acyl-sn-glycerophosphorylethanolamine, or PE (each was dispersed at 0.5% [w/v] in 0.02% Tween 20; data not shown). Plant hormones, such as 2 μ M brassinolide or 5 μ M 2,4-D, were also ineffective (data not shown). By contrast, the abnormalities could be rectified by cosegregation with either *transPECT1* (Figure 5A) or wild-type *PECT1* cDNA under the control of *Pro_{35S}* (Figure 5B), suggesting a causal relationship between *PECT1* and the pleiotropic abnormalities in *pect1-4/pect1-6* F1 plants. In a transgenic *pect1-4/pect1-6* F1 line containing a *PECT1* cDNA under the control of an estrogen-inducible promoter (Zuo et al., 2000), local application of estrogen (0.1 mM 17 β -estradiol) on rosette leaves partially relieved the dwarfism and early senescence of the transheterozygotic mutants (Figure 5C). However, flowers of the transgenic *pect1-4/pect1-6* F1 line resembled fertile flowers of nontransgenic *pect1-4/pect1-6* F1 plants, even if estrogen was applied to the whole plant. These results for *pect1-4/pect1-6* F1 plants suggest that malfunctions in different tissues have a synergistic effect on the mutant phenotypes.

Expression Profiles of *PECT1* in Intact Tissues

To examine the expression profiles of *PECT1* in intact tissues, transgenic *Arabidopsis* lines expressing either enhanced yellow fluorescent protein (EYFP)-tagged *PECT1* under the control of

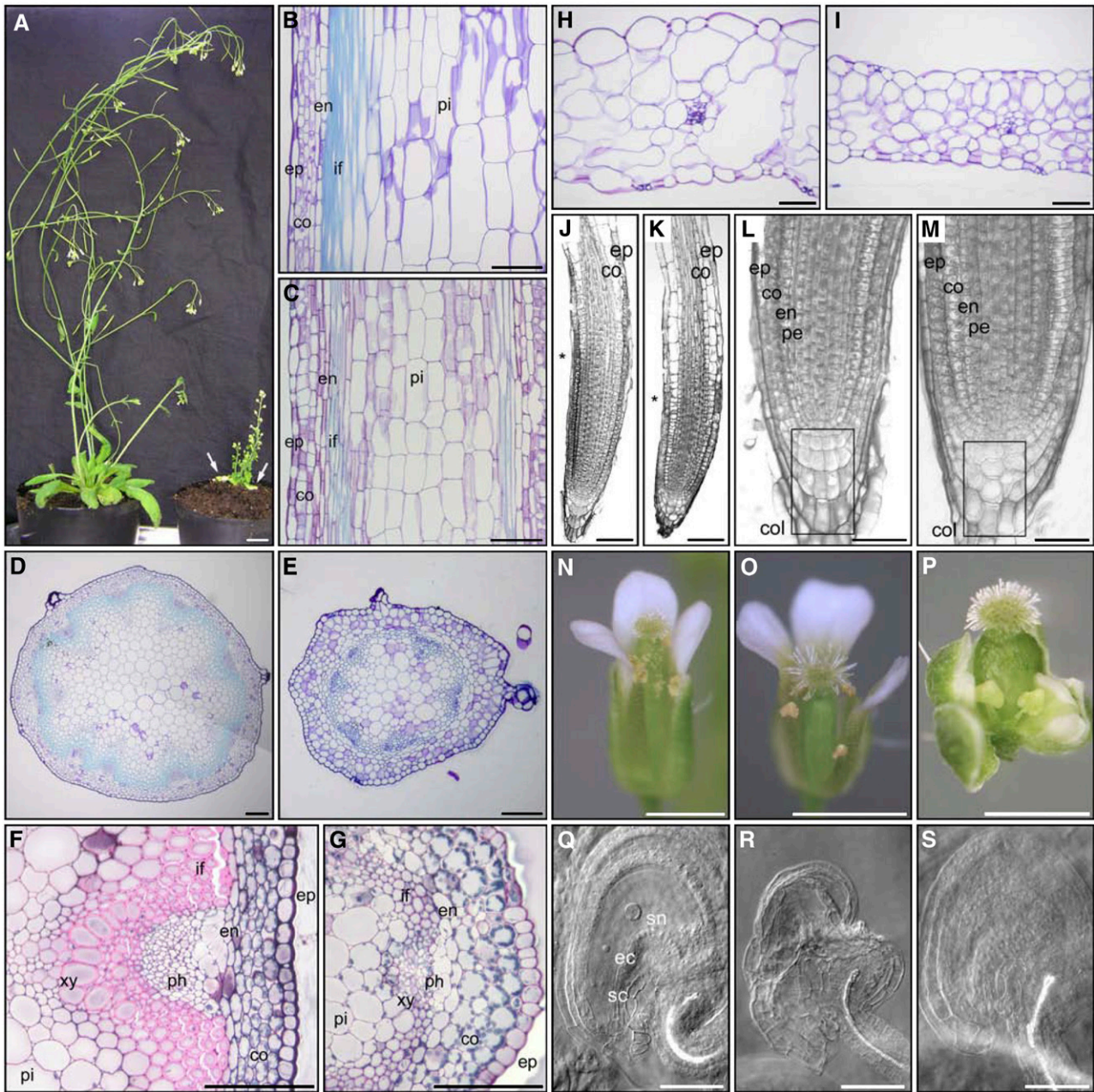


Figure 4. Mutant Phenotypes of *pect1-4/pect1-6* F1 Plants.

(A) Forty-day-old wild-type (left) and *pect1-4/pect1-6* F1 (right) plants.

(B) and **(C)** Toluidine blue–stained longitudinal sections of the bases of mature major stems from wild-type **(B)** and *pect1-4/pect1-6* F1 **(C)** plants.

(D) and **(E)** Toluidine blue–stained transverse mature stem sections from wild-type **(D)** and *pect1-4/pect1-6* F1 **(E)** plants.

(F) and **(G)** Triple-stained transverse mature stem sections from wild-type **(F)** and *pect1-4/pect1-6* F1 **(G)** plants.

co, cortex; en, endodermis; ep, epidermis; if, interfascicular fibers; ph, phloem; pi, pith; xy, xylem.

(H) and **(I)** Toluidine blue–stained transverse mature leaf sections from wild-type **(H)** and *pect1-4/pect1-6* F1 **(I)** plants. Sections were made across the fifth true leaves of 20-d-old plants that had just bolted.

(J) and **(K)** Toluidine blue–stained root tips from wild-type **(J)** and *pect1-4/pect1-6* F1 **(K)** seedlings. Asterisks indicate the position of an assumed boundary between the meristematic and elongation zones.

(L) and **(M)** Higher magnification images of root tips from wild-type **(L)** and *pect1-4/pect1-6* F1 **(M)** seedlings. col, columella; pe, pericycle.

(N) to **(P)** A wild-type flower **(N)** is shown together with mutant flowers from *pect1-4/pect1-6* F1 plants with moderate **(O)** and severe **(P)** stamen mutations. Sepals and petals are partially removed.

(Q) A wild-type unfertilized ovule with a normal embryo sac. ec, egg cell; sc, synergid cells; sn, secondary nucleus.

(R) and **(S)** A *pect1-4/pect1-6* silique containing abnormal unfertilized ovules with either withered morphology **(R)** or lacking embryo sac development **(S)**.

Bars = 1 cm for **(A)**, 100 μ m for **(B)** to **(K)**, 50 μ m for **(L)**, **(M)**, and **(Q)** to **(S)**, and 1 mm for **(N)** to **(P)**.

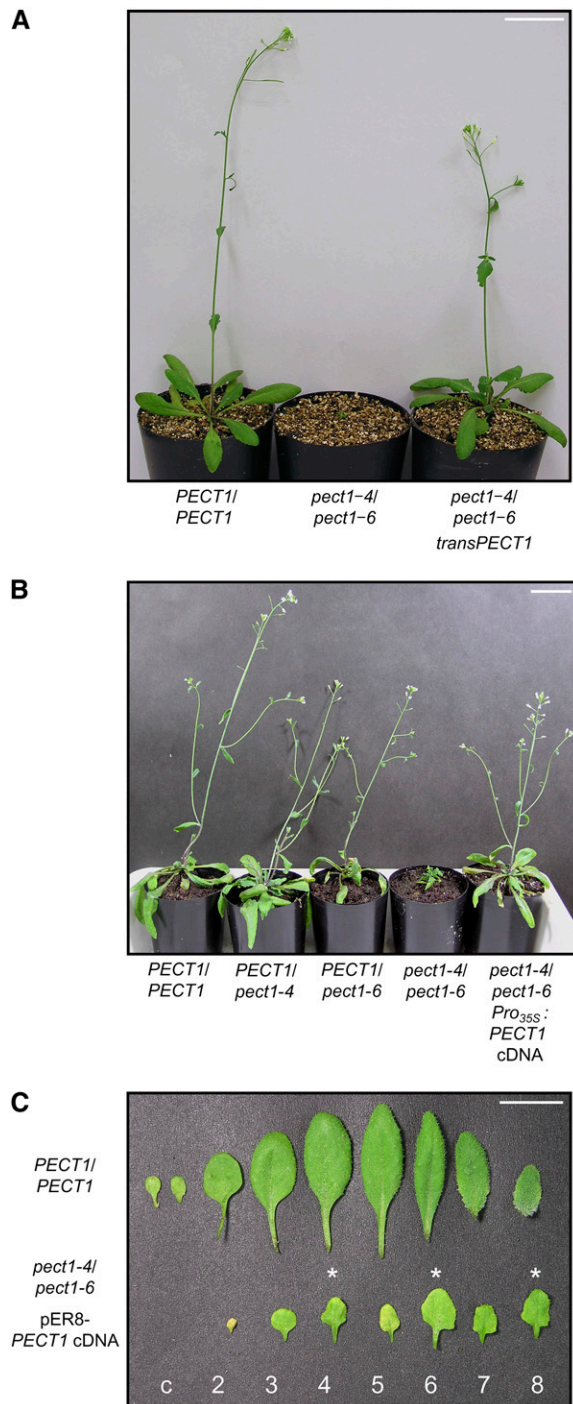


Figure 5. Normalization of Growth Defects in *pect1-4/pect1-6* F1 Plants by Transgene Expression.

(A) A *pect1-4/pect1-4 transPECT1*^{-/-} plant was crossed with a *PECT1/pect1-6* plant. In the F1 progeny, all *pect1-4/pect1-6* plants with no *transPECT1* (middle; 3 of 26) exhibited dwarfism, whereas all *pect1-4/pect1-6* plants with *transPECT1* (right; 8 of 26) had a normal appearance. The photograph was taken after 30 d under continuous illumination at 23°C.

(B) A *PECT1/pect1-4 Pro_{35S}:PECT1 cDNA*^{-/-} plant was crossed with a

Pro_{PECT1} or EYFP under the control of *Pro_{35S}* were created and designated PECT1-EYFP and 35S-EYFP, respectively. Fluorescence from these lines was compared with an epifluorescence microscope. Although all tissues of PECT1-EYFP seedlings emitted background fluorescence, the strongest fluorescent signal was observed in emerging true leaves and shoot apices (Figure 6A). By contrast, 35S-EYFP seedlings emitted only background fluorescence (Figures 6A and 6B). In roots, the strongest fluorescence was observed in the regions 200 to 500 μm beneath the root tip in the PECT1-EYFP seedlings (Figure 6C) versus just beneath the root tip in 35S-EYFP seedlings (Figure 6D). Developing lateral root primordia in PECT1-EYFP seedlings also fluoresced robustly compared with stele tissues (Figure 6E), but fluorescence from these tissues was equally strong in 35S-EYFP seedlings (Figure 6F). In transverse sections of just-bolted stems, vascular bundle fluorescence was prominent in PECT1-EYFP plants (Figure 6G) compared with background fluorescence in 35S-EYFP plants (Figure 6H). The strongest fluorescence in PECT1-EYFP plants was in the central region of pollen grains (Figure 6I). By contrast, no fluorescence was detected in the pollen of 35S-EYFP plants (Figure 6J). Confocal laser scanning microscopy revealed strong fluorescence from globular-stage embryos in the siliques of PECT1-EYFP plants 3 d after flowering (Figure 6K). Together, these results suggest that *PECT1* expression is greatest in tissues undergoing cell division or elongation.

Subcellular Localization of PECT1-EYFP

In plants expressing PECT1-EYFP, small fluorescent particles were observed within cells of roots, hypocotyls, cotyledons, petals, and stamen filaments. Fluorescence did not overlap with chlorophyll autofluorescence in the cotyledons and petals, suggesting that these particles represent mitochondria (Figures 6L to 6O). Root epidermal cells of PECT1-EYFP and 35S-EYFP seedlings were stained with a fluorescent mitochondrial dye, MitoTracker Red CMXRos (Figures 6Q and 6T, respectively). The small ring-like structures representing PECT1-EYFP fluorescence (Figure 6P) were superimposable with MitoTracker-stained mitochondria (Figure 6R). The ring-like image of PECT1-EYFP fluorescence was enhanced by superimposing the images. By contrast, EYFP fluorescence in root epidermal cells of 35S-EYFP

PECT1/pect1-6 plant. In the F1 progeny, no *pect1-4/pect1-6* plants expressing *Pro_{35S}:PECT1* cDNA exhibited dwarfism. The photograph was taken after 30 d under continuous illumination at 23°C.

(C) Transheterozygotes display severe fertility defects, and thus a *pect1-4/pect1-6 transPECT1*^{-/-} plant carrying an estrogen-inducible *PECT1* cDNA under the control of an estrogen-inducible promoter was created (Zuo et al., 2000). Of the ~100 offspring of the transgenic plant, three independent *pect1-4/pect1-6* F1 plants carrying an estrogen-inducible *PECT1* cDNA were identified. For one plant, 0.1 mM estrogen solution was applied onto the fourth, sixth, and eighth true leaves (asterisks), whereas control DMSO solution was applied onto the third, fifth, and seventh leaves. Estrogen-treated rosette leaves are larger than control leaves and exhibit less senescence (cf. the fourth and fifth leaves). Numbers indicate leaf positions, and c indicates cotyledons. Bars = 5 cm in **(A)** and **(B)** and 1 cm in **(C)**.

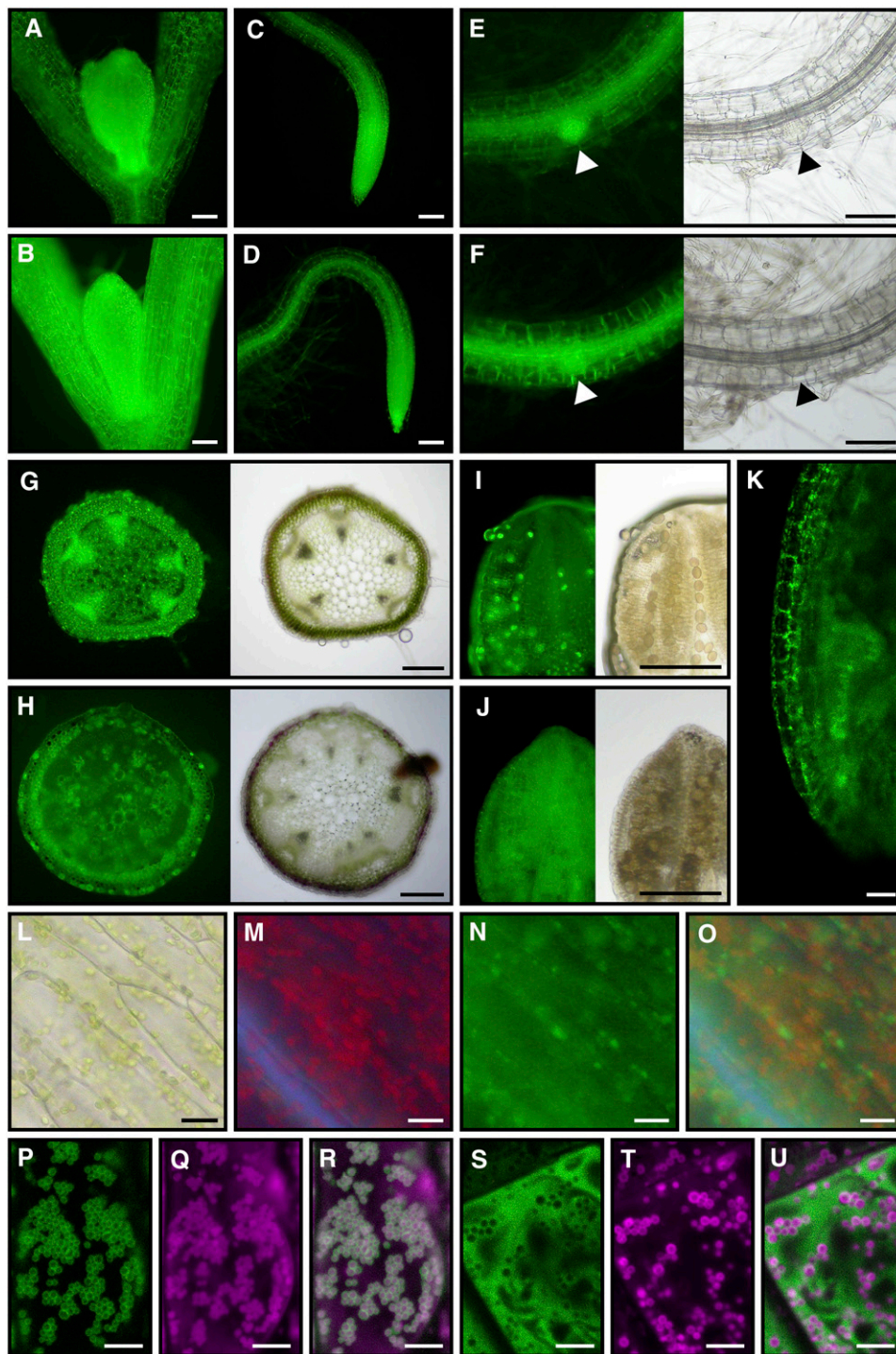


Figure 6. Fluorescence Images of Various Tissues from Transgenic PECT1-EYFP and 35S-EYFP Plants.

Images representing more than four independent transgenic lines are shown.

(A) and **(B)** Images of shoot apices of 5-d-old PECT1-EYFP **(A)** and 35S-EYFP **(B)** plants.

(C) and **(D)** Images of root apices of 5-d-old PECT1-EYFP **(C)** and 35S-EYFP **(D)** plants.

(E) and **(F)** Fluorescence (left) and bright-field (right) images of the developing lateral root primordia (indicated by arrowheads) of PECT1-EYFP **(E)** and 35S-EYFP **(F)** seedlings.

(G) and **(H)** Fluorescence (left) and bright-field (right) images of transverse stem sections from PECT1-EYFP **(G)** and 35S-EYFP **(H)** plants that had just bolted.

seedlings (Figure 6S) did not overlap with MitoTracker-stained mitochondria (Figure 6U). These results indicate that, in *Arabidopsis*, PECT1 is localized around the periphery of mitochondria, most likely in the mitochondrial membrane.

Lipid Composition of *pect1* Plants

Total lipids were extracted from rosette leaves of wild-type, *pect1-4/pect1-4*, *pect1-4/pect1-6*, and *pect1-4/pect1-6 transPECT1/-* plants for quantification of lipid classes, as described in Methods. In rosette leaves, PE levels were decreased from 11.4% in wild-type plants to 7.4% in *pect1-4/pect1-6* F1 plants (a 35.1% reduction). The proportion of monogalactosyldiacylglycerol was also decreased, whereas PC was increased, in transheterozygotic plants (see Supplemental Figure 2A online). In addition, the proportions of palmitate (16:0) in digalactosyldiacylglycerol (DGDG), phosphatidylglycerol, and PC were increased in transheterozygotic plants (boldface figures in Supplemental Table 11 online). However, there was no significant change in the fatty acid composition of the other polar glycerolipids (see Supplemental Table 11 online). In rosette leaves of *pect1-4/pect1-4* plants, PE levels decreased only slightly from 11.4% in the wild type to 10.5% (~8% reduction). The difference was enhanced when the lipid composition of etiolated seedlings was compared (see Supplemental Figure 2B online). PE content was reduced by ~20%, from $20.9 \pm 1.0\%$ in the wild type to $16.6 \pm 1.2\%$ in *pect1-4* seedlings.

In a transgenic *pect1-4/pect1-6 transPECT1/-* F1 plant, PE and PC levels as well as the fatty acid composition of PC and DGDG were equivalent to those in the wild type. However, monogalactosyldiacylglycerol and 16:0-phosphatidylglycerol levels recovered by ~30 and ~10%, respectively, indicating that these changes may not be completely related to *pect1* mutations. Dramatic differences in PE content between *pect1-4* and *pect1-4/pect1-6* mutants suggest that there is a threshold level of PECT activity required to maintain optimal PE biosynthesis via the CDP-Etn pathway in *Arabidopsis*.

DISCUSSION

Amino Acid Residues That May Be Functionally Important for PECT Proteins

Table 1 summarizes the *pect1* alleles identified from the TILLING analysis. *pect1-2*, *pect1-3*, *pect1-4*, and *pect1-9* alleles reduced PECT activity in rosette leaf homogenates (Figure 1B), providing

information about amino acid residues critical for PECT function. The potential significance of each of these residues is discussed below; however, determination of the exact function of these residues will require kinetic and crystallographic analyses of recombinant PECT1 proteins. The *pect1-2* allele decreased PECT activity by 21% as a result of an A96V substitution, although the Ala-96 residue is not conserved in any known PECT proteins other than those in angiosperms. The *pect1-3* and *pect1-4* alleles reduced PECT activity by 21 and 74%, respectively. Both Pro-101 (*pect1-3*) and Pro-126 (*pect1-4*) are located within the first catalytic domain, and they are conserved among all PECTs in the databases, suggesting that these Pro residues are involved in the catalytic function of PECTs. However, it is also possible that Pro-to-Ser conversions cause a significant conformational change in PECTs. The *pect1-9* allele reduced PECT activity by 46% as a result of an S232L substitution. This residue is also conserved among known mammalian PECTs, but it is located between the two conserved catalytic domains, making a conformational role possible.

Embryonic Development Is Susceptible to Limited PECT Activity

PECT1/pect1-6 plants are normal in all aspects of plant development, suggesting that a single copy of *PECT1* (i.e., 50% of wild-type PECT activity) is sufficient for proper embryonic and postembryonic development of *Arabidopsis*. Embryonic development is delayed in homozygous, but not heterozygous, *pect1-4* plants. These homozygous mutants display ~25% of wild-type PECT activity (Figure 3F). Ovules of *PECT1/pect1-4* plants generally appear normal (see Supplemental Table 6 online); therefore, embryonic or endospermic *pect1-4* must underlie the maturation delays. Seed abortion rates are increased in *pect1-4/pect1-6* F1 plants, which exhibit ~20% of wild-type PECT activity (see Supplemental Table 8 online). *pect1-6* embryos cannot develop beyond the octant stage when borne in *PECT1/pect1-6* ovules (Figure 2), suggesting that embryonic or endospermic *pect1-6* is responsible for early embryonic lethality. In summary, a reduction in embryonic or endospermic PECT activity likely impedes embryonic development in *Arabidopsis*. Thus, the widely varying population of *pect1-4* embryos observed during development and the partial lethality of *pect1-4/pect1-6* embryos likely reflect either the incomplete penetrance of mutant phenotypes or variations in PECT activity among different seeds or siliques.

Figure 6. (continued).

(I) and (J) Fluorescence (left) and bright-field (right) images of anthers from PECT1-EYFP (I) and 35S-EYFP (J) plants.

(K) A confocal image of an embryo in a developing seed of a PECT1-EYFP plant.

(L) to (O) Higher magnification images of a petal from a PECT1-EYFP plant. A bright-field image (L), an autofluorescence image (M), and a PECT1-EYFP image (N) are shown. An overlay of (M) and (N) is shown in (O).

(P) to (R) Confocal images of root epidermal cells from a PECT1-EYFP plant. Fluorescence images of PECT1-EYFP (P), MitoTracker Red (Q), and the overlay (R) are shown.

(S) to (U) Confocal images of root epidermal cells from a 35S-EYFP plant. Fluorescence images of 35S-EYFP (S), MitoTracker Red (T), and the overlay (U) are shown.

Bars = 100 μ m for (A) to (J), 10 μ m for (K) to (O), and 5 μ m for (P) to (U).

According to the SeedGenes database (<http://www.seedgenes.org/>) (Tzafrir et al., 2003), to date, 253 independent *Arabidopsis* gene mutations have been identified that cause embryonic lethality. However, only 56 genes (22%) produce embryonic lethality before the globular stage. In a comprehensive analysis of 23 embryonic lethal mutants whose phenotypes have been confirmed by more than two independent alleles, only three genes are related to lethality at preglobular stages (Tzafrir et al., 2004). Our results show that *PECT1* is a new member of this small group of genes.

The CDP-Etn Pathway Is Crucial for PE Synthesis in *Arabidopsis*

In yeast, PS decarboxylation is the major pathway of PE biosynthesis, and *psd1Δ psd2Δ* mutants devoid of this pathway generate respiration-deficient cells called petite cells (Birner et al., 2001). These double mutants cease growth on medium containing only nonfermentable carbon sources. PE levels in *psd1Δ psd2Δ* mutants decrease to 1% before cell growth arrest, whereas wild-type cells maintain PE at 18% (Birner et al., 2001). PE shortage does not, however, lead to cell death for at least 4 d. When Etn is supplied to the double mutant cells, the PE level increases to ~3%, but growth rates do not recover to wild-type levels. Therefore, limiting PE biosynthesis causes mitochondrial malfunction in yeast (Birner et al., 2001).

In a mutant Chinese hamster ovary cell line, CHO-K1 R-41, a malfunction of the PS decarboxylation pathway reduces PE synthesis. Cellular PE levels decrease from 18% in the wild type to 9% in R-41 cells. R-41 cells can grow in medium supplemented with Etn, the substrate of the CDP-Etn pathway of PE synthesis. Although cell growth is not fully supported without Etn, R-41 cells increase fivefold in number before growth cessation, whereas PE levels relative to total phospholipids decrease by 38% (Emoto and Umeda, 2000). Therefore, there must be a threshold PE level required for cell proliferation. In this cell line, disassembly of contractile rings at the cleavage furrow of dividing cells requires PE (Emoto and Umeda, 2000).

In *Arabidopsis*, the first division of zygotes produces two sister cells destined to become the suspensor and embryo proper. Accordingly, a *pect1-6* zygote must divide four times to become an octant-stage embryo. How is this accomplished by the *pect1-6* zygote that lacks functional *PECT1*? PE could be synthesized from endogenous PS via the aforementioned PS decarboxylation or base-exchange pathway. *CHO1* encodes the major PS synthase in yeast, CDP-diacylglycerol:serine phosphatidyltransferase (Kiyono et al., 1987). However, no *CHO1* ortholog exists in *Arabidopsis* (see the Arabidopsis Lipid Database at Michigan State University: <http://www.plantbiology.msu.edu/lipids/genesurvey/>), suggesting that in *Arabidopsis* PS must be synthesized from PE via the base-exchange pathway. Thus, a dilemma is created. In *Arabidopsis*, PE synthesis via PS decarboxylation requires PS formation via the base-exchange pathway, which in turn requires PE synthesis via the CDP-Etn pathway. Therefore, it seems unlikely that PS decarboxylation or base exchange could compensate for defects in the *Arabidopsis* CDP-ethanolamine pathway. The seed-abortion phenotype of *pect1-6* embryos is consistent with this view. However,

the biosynthesis of PE via the CDP-Etn pathway seems to be dispensable in pollen. The role of other PE biosynthesis pathways in male reproductive organs should be examined in future research.

PECT1 mRNA, its translation product, or its reaction product, CDP-Etn, could be meiotically transferred from the mother cell to *pect1-6* zygotes. Such transmission would provide a mechanism to support minimal cell division in *pect1-6* zygotes. However, in hemizygous *PECT1*-EYFP flowers, nonfluorescent pollen grains were as frequent as strongly fluorescent pollen grains (Figure 6I), indicating that meiotic transmission of *PECT1*-EYFP protein or its mRNA is insignificant, at least to male gametophytes. Therefore, the amount of PE remaining in the zygote is likely rate-limiting for *pect1-6* embryo development.

Local Lipid Changes May Underlie the Mutant Phenotypes

In *Arabidopsis*, unlike mammals, limiting lipid-synthesizing activity causes severe dwarfism but only minor changes in the lipid content (Xu et al., 2006). There is the possibility that other biosynthetic pathways complement the defect of the CDP-Etn pathway. However, our RT-PCR experiments showed that none of the transcripts for *PSS1*, *PSD1*, *PSD2*, and *PSD3* changed significantly in *pect1-4* plants compared with wild-type plants (data not shown).

The effect of *pect1-4* on PE content is partially masked in rosette leaves as a result of the presence of chloroplasts, which contain abundant glycolipids. As such, the *pect1-4* mutation decreases PE content by 20.6 and 7.9% in etiolated seedlings and rosette leaves, respectively. Thus, we predict that the PE content of etiolated *pect1-4/pect1-6* seedlings is more severely affected than that of *pect1-4/pect1-6* rosette leaves, which exhibit a 35% reduction. However, etiolated *pect1-4/pect1-6* seedlings are currently not available in numbers sufficient for lipid analyses.

The reciprocal increase in PC content (see Supplemental Figure 2 online) observed concurrently with the PE decrease may be a compensatory mechanism, because diacylglycerols for PE biosynthesis as well as phosphorylethanolamine, from which CDP-choline is derived, can be recruited for PC biosynthesis in *Arabidopsis*. In addition, increased levels of 16:0 in PC and DGDG are closely related, because PC serves as a DGDG precursor in plants. Although these types of lipid changes could directly cause the mutant phenotypes observed in *pect1-4/pect1-6* F1 plants, we demonstrate that the *pect1* mutation and the associated reduction of PE content (or CDP-Etn content) cause these lipid changes. Therefore, it will be important to investigate which cellular compartments are affected by the lipid changes.

Analysis of mitochondrial membrane lipids is of primary importance. PE is the major lipid in mitochondria, and mitochondrial malfunction causes enormous damage to cells. PE is also essential for a number of other membranes and proteins. PE is required for glycosylphosphatidylinositol-anchored protein synthesis (Menon and Stevens, 1992), and thus decreased PE content in Golgi membranes may result in the delayed maturation of glycosylphosphatidylinositol-anchored proteins (Birner et al., 2001). Vacuolar membranes are also an important target. In

intact cells, cytoplasmic components such as organelles travel dynamically through transvacuolar strands (Saito et al., 2005). Judging by their shape, construction of such membrane strands may require nonbilayer lipids such as PE. Therefore, a shortage of PE may affect dynamic vacuolar functions. Further analysis of lipids and mutant phenotypes in various cellular compartments will require callus or cell suspension cultures, and we are currently trying to establish such cultures from *pect1-4/pect1-6* transheterozygotes.

Mitochondrial Localization of PECT1

In rat (*Rattus norvegicus*) hepatocytes, PECT proteins localize to the cytoplasm and the endoplasmic reticulum membrane (van Hellemond et al., 1994). In yeast, localization of PECT proteins remains to be determined, although they are hydrophilic (Bladergroen and van Golde, 1997). By contrast, PECT activity has been reported in the endoplasmic reticulum membrane and the cytoplasmic face of purified mitochondria in castor bean (*Ricinus communis*) endosperms (Wang and Moore, 1991). The PECT precursor in *Chlamydomonas reinhardtii* is also predicted to contain a mitochondrial targeting signal (Yang et al., 2004). Proteome analysis of purified mitochondria from *Arabidopsis* suggests that PECT1 is mitochondrially associated (Heazlewood et al., 2004). Here, we find that EYFP-tagged PECT1 localizes at the mitochondrial periphery, most likely in the outer membrane (Figures 6P to 6R).

Based on Target P searches (Emanuelsson et al., 2000), the Arabidopsis Lipid Database at Michigan State University (<http://www.plantbiology.msu.edu/lipids/genesurvey/>) predicts that PECT1 is a secretory pathway enzyme that is processed to yield a mature 43-kD protein. However, our immunoblot analysis detected an ~47-kD PECT1 band, suggestive of unprocessed protein. We note, however, that PECT1 may run anomalously during SDS-PAGE. A signal peptidase recognition site is not required for mitochondrial targeting of some proteins (Koehler, 2004). Furthermore, little is known about the mechanisms governing protein targeting to outer mitochondrial surfaces. Therefore, the database prediction that there is no cleavage site for mitochondrial signal peptidases is compatible with our view that PECT1 localizes in the outer mitochondrial membrane. Thus, we think it unlikely that PECT1 localizes to other cellular compartments, but this point requires further investigation.

The Utility of *pect1* TILLING Mutants for the Analysis of PE Function in *Arabidopsis*

Swollen-cell phenotypes are observed in various tissues and cell types of *pect1-4/pect1-6* F1 plants. Cell swelling occurs when the cell wall cannot support normal turgor pressure. Inhibition of cellulose synthesis (Hogetsu et al., 1974; Baskin and Bivens, 1995; Nicol et al., 1998; Beeckman et al., 2002) or assembly of cellulose fibrils (Burk et al., 2001) causes cell swelling (Figures 4E and 4G). Therefore, in this regard, it should be informative to compare the cell wall composition and/or orientation of cellulose microfibrils in *pect1-4* and *pect1-4/pect1-6* F1 plants. The mature rosette leaves of transheterozygotic plants also develop mesophyll cells with few intercellular spaces (Figure 4I). Larger

intercellular spaces in wild-type plants may be the result of cell wall loosening between neighboring cells and subsequent cell expansion. Therefore, future research should address putative processes that relate protein secretion to cell wall modification or cell expansion.

Cell viability is orchestrated by various organelles that change dynamically under various physiological conditions. In this regard, modern technologies such as confocal laser scanning microscopy and fluorescently tagged organelle markers permit the study of dynamic functions of plant organelles. The significance of changes in PE levels in response to environmental cues and the mechanism of intracellular PE translocation remain undefined, but our mutants provide a useful genetic background for these studies.

METHODS

Plant Materials and Growth Conditions

Seeds of *Arabidopsis thaliana*, ecotype Columbia, were obtained from Lehle Seeds and sown on peat sheets (Sakata Seed) irrigated with water. After vernalization at 2°C for 2 d in darkness, seedlings were raised at 23°C under continuous illumination at a photon flux density of 75 $\mu\text{mol}\cdot\text{m}^{-2}\cdot\text{s}^{-1}$. Unless noted otherwise, 18-d-old seedlings from wild-type and mutant plants were used for experiments just before bolting. *pect1-4/pect1-6* F1 seedlings were grown for ~30 d under the same conditions. For observation of hypocotyls and roots, surface-sterilized seeds were sown on 0.9% agar medium containing half-strength Murashige and Skoog salts (Murashige and Skoog, 1962), Gamborg B5 vitamins (Gamborg et al., 1968), 1% sucrose, and 0.05% MES, pH 5.7. After vernalization at 2°C for 2 d in darkness, agar plates were incubated in a vertical position for 6 d at 23°C under the same photon flux density described above. For lipid analyses of etiolated seedlings, sterilized seeds were placed in 300-mL flasks containing 50 mL of a medium consisting of half-strength Murashige and Skoog salts, Gamborg B5 vitamins, 1.5% sucrose, and 0.05% MES, pH 5.7. They were then chilled at 2°C for 2 d in darkness for vernalization and germinated at 23°C for 3 d under continuous light with gentle shaking (30 rpm). Then, another 50 mL of the medium was supplied and germinated seedlings were grown for an additional 11 d at 23°C in darkness to obtain etiolated seedlings. Mutant seeds and the BAC clone were obtained from the ABRC at Ohio State University. Finally, it should be noted that because *pect1-4* plants showed reduced fertility, careful control was required to maintain this line. Measures were taken to eliminate accidental cross-pollination of *pect1-4* plants, and genotyping was performed before each experiment as described below.

TILLING Searches for *pect1* Alleles

Allelic *pect1* mutants were isolated from a pool of ethyl methanesulfonate-induced mutant seeds obtained from the ABRC with the aid of the TILLING project (Till et al., 2003). The primers PECT1/121F (5'-GGTTGTCTTGTCCATGGCGCATT-3') and PECT1/1091R (5'-GCTCAGACTCTCAGAGCCCTTGC-3') were used for the TILLING search. Homozygous *pect1-2*, *pect1-3*, and *pect1-9* mutants were selected after a single backcross with the wild type, whereas the heterozygous *PECT1/pect1-4* mutant was backcrossed three times with the wild type before the homozygous mutant could be isolated. The *pect1-6* mutation was maintained in heterozygous *PECT1/pect1-6* plants, which were backcrossed at least three times with the wild type before use. The *er-105* mutation in the original seeds was segregated during the purification of all mutant alleles. Accession numbers for the identified *pect1* alleles at The Arabidopsis Information Resource (<http://www.arabidopsis.org/>) are shown in Table 1.

Production of *pect1-4/pect1-6* F1 Plants

Transheterozygotes were generated most efficiently by crossing male gametophytes from *pect1-4/pect1-4* plants and female gametophytes from *PECT1/pect1-6* plants. The resultant *pect1-4/pect1-6* seeds were easily identified by their small size relative to *PECT1/pect1-4* seeds.

Production of Transgenic Plants

For expression of a foreign *PECT1* gene fragment in *Arabidopsis*, a 6.5-kb *Bam*HI-*Sac*I *PECT1* fragment, designated *transPECT1*, was prepared from the BAC clone T6A23 and subcloned into the binary vector pPZP21 (Hajdukiewicz et al., 1994), a generous gift from Pal Maliga at Rutgers University. The resultant Ti plasmid was designated pPZP21-*transPECT1*. The *transPECT1* gene contained a 0.5-kb promoter region (*Pro*_{*PECT1*}) and a 2.5-kb 3' noncoding region of the *PECT1* gene.

To construct a Ti plasmid for ectopic expression of *PECT1* cDNA, a *PECT1* cDNA fragment was amplified by PCR from a cDNA pool derived from *Arabidopsis* rosette leaf mRNAs using the primers 5'*PECT*sen (5'-AAACCCGGGATGGTTGGGAGAAAGAGAAG-3') and 3'*PECT*sen (5'-AAAGAGCTCTCAGTCTCCGGAACAAACGA-3'). The resultant PCR fragment was subcloned between the *Sma*I and *Sac*I sites of pBluescript II KS+ (Stratagene) for sequence confirmation. *Sma*I-*Sac*I fragments of *PECT1* cDNA were then subcloned between the cauliflower mosaic virus 35S promoter (*Pro*_{35S}) and the nopaline synthase (*NOS*) terminator (*Ter*_{*NOS*}) of the plasmid pBI221 (Becton Dickinson). The resultant *Pro*_{35S}:*PECT1* cDNA:*Ter*_{*NOS*} cassette was subcloned between the *Pst*I and *Eco*RI sites of pPZP21. The plasmid was designated pPZP21-*Pro*_{35S}:*PECT1* cDNA:*Ter*_{*NOS*}.

The Ti plasmid for expression of *PECT1* cDNA under the control of an estrogen-inducible promoter was produced by subcloning a *PECT1* cDNA into the Ti plasmid pER8 (Zuo et al., 2000), obtained from N.-H. Chua at The Rockefeller University. A *PECT1* cDNA fragment was excised from pQE30-*PECT1* (see below) by *Bam*HI and *Pst*I and then subcloned into the *Xho*I site of pER8 by blunt-end ligation. The resulting Ti plasmid was designated pER8-*PECT1*. *pect1-4/pect1-6 transPECT1/-* plants were first transformed with pER8-*PECT1*. A *pect1-4/pect1-6 transPECT1/-* plant carrying the estrogen-inducible *PECT1* cDNA was then isolated by antibiotic resistance and genotype analysis. Three *pect1-4/pect1-6* plants carrying the estrogen-inducible *PECT1* cDNA were isolated among the offspring.

To generate Ti plasmids for expression of EYFP or a *PECT1*:EYFP fusion, an EYFP fragment from the pEYFP-N1 plasmid (Becton Dickinson) was subcloned into the *Bam*HI and *Not*I sites of pBluescript II KS+, then excised as a *Bam*HI-*Sac*I fragment. This fragment was subcloned into pBI221 in place of the β -glucuronidase gene. The resultant *Pro*_{35S}:EYFP:*Ter*_{*NOS*} cassette was subcloned between the *Hind*III and *Eco*RI sites of the binary vector pPZP211 to obtain the pPZP211-*Pro*_{35S}:EYFP:*Ter*_{*NOS*} plasmid. Another *PECT1* cDNA fragment was amplified by PCR using primers *PECT1/N-Bam*HI (5'-AAAGATCCATGGTTGGGAGAAAGAGAAG-3') and *PECT1/2701R-Bam*HI (5'-AAGGATCCGTCCTCCGGACAAACGAC-3'). The resulting *PECT1* cDNA fragment was subcloned into the *Bam*HI site of pPZP211-*Pro*_{35S}:EYFP:*Ter*_{*NOS*} to produce pPZP211-*Pro*_{35S}:*PECT1*cDNA:EYFP:*Ter*_{*NOS*}. Finally, a 3.8-kb *Hind*III fragment of *Pro*_{*PECT1*}:*PECT1* from pPZP211-*transPECT1* was subcloned into pPZP211-*Pro*_{35S}:*PECT1*cDNA:EYFP:*Ter*_{*NOS*} in place of the *Hind*III fragment of *Pro*_{35S}:*PECT1*cDNA to construct the pPZP211-*Pro*_{*PECT1*}:*PECT1*:EYFP:*Ter*_{*NOS*} plasmid.

All plants were transformed by the floral dip method (Clough and Bent, 1998) using *Agrobacterium tumefaciens* EHA101. Transgenic lines with a single T-DNA insertion were segregated by antibiotic resistance.

pect1-4/pect1-4 transPECT1/- plants were isolated from the F2 progeny of a cross between *PECT1/pect1-4* and *transPECT1/-* plants.

Genotyping of Mutants and Transgenic Plants

Siliques were opened 6 d after flowering, and embryo size was recorded for each developing seed. Each embryo was then dissected from the seed with the use of a dissecting microscope and a pair of tweezers. Dissected embryos were rinsed once with 500 μ L of a buffer containing 10 mM Tris-HCl, pH 8.0, and 1 mM EDTA and then subjected to DNA extraction. DNA samples were genotyped as described below.

DNA was extracted from either young cotyledons or rosette leaves to genotype seedlings. Leaf samples were homogenized in an extraction buffer containing 0.2 M Tris-HCl, pH 9.0, 0.4 M LiCl, 25 mM EDTA, and 1% SDS. Homogenates were then extracted with an equal volume of phenol:chloroform:isoamyl alcohol (25:24:1, v/v), followed by a chloroform extraction. DNA was precipitated by adding an equal volume of isopropyl alcohol.

pect1-2 and *pect1-9* mutations were detected with a simple CAPS analysis. *pect1-3*, *pect1-4*, and *pect1-6* mutations were identified by dCAPS analysis (Neff et al., 1998). To discriminate the *transPECT1* gene from endogenous *PECT1*, the latter gene was identified by dCAPS analysis. Primers and enzymes used for these analyses are summarized in Supplemental Table 12 online.

Estrogen Treatment of Transgenic Plants

After genotype determination, transgenic *pect1-4/pect1-6* F1 plants carrying a *PECT1* cDNA under the control of an estrogen-inducible promoter were treated with estrogen. Just before use, a 20 mM stock solution of 17 β -estradiol (biochemical grade; Wako Pure Chemical Industries) in DMSO was diluted with 0.02% (v/v) Tween 20 to yield a final concentration of 0.1 mM. Estradiol (0.1 mM) was applied to the surface of rosette leaves as small droplets. DMSO (0.5%, v/v) in 0.02% (v/v) Tween 20 was applied in a similar manner to control leaves. These treatments were performed every day after the sixth rosette leaves became visible in the rosette centers of transheterozygotic seedlings.

Measurements of PECT Activity

PECT activity in *Arabidopsis* rosette leaves was measured according to a method for measuring CTP:phosphorylcholine cytidyltransferase activity (Inatsugi et al., 2002), except the reaction was conducted at pH 8.5 using [1,2-¹⁴C]phosphorylethanolamine (83.25 kBq/mmol; American Radiolabeled Chemicals) as a substrate in place of phosphoryl [methyl-¹⁴C] choline. The reaction (20 μ L) contained 100 mM Tris-HCl, pH 8.5, 5 mM CTP (C1506; Sigma-Aldrich), 25 mM MgCl₂, 5 mM DTT, and 4 mM [1,2-¹⁴C]phosphorylethanolamine. Leaf homogenates equivalent to 1.25 to 2.5 mg of fresh leaves were added to initiate the reaction. The reaction was then maintained for 30 min at 25°C before the addition of a stop solution (10 μ L) containing 10% (w/v) trichloroacetic acid and 10 μ g of CDP-ethanolamine. A 10- μ L aliquot was then streaked 10 mm in width onto a silica gel 60 plate (No. 1.05721.0009; Merck). The plate was developed using a solvent mixture of ethanol:2.5% ammonia (3:2, v/v). Radioactive bands were detected and quantified using a Bio-Imaging analyzer (BAS2000; Fuji Photo Film).

Determination of Nucleotide Sequences

Nucleotide sequences were determined using a DNA sequencer (4000L; Li-Cor).

Preparation of an Anti-PECT1 Antiserum

Rabbit antiserum against PECT1 was prepared by Sawady Technology. The antigen was recombinant PECT1 with an N-terminal six-His tag (6 \times His-PECT1) expressed in *Escherichia coli* M15 [pREP4]. A *PECT1*

cDNA fragment was amplified by PCR from the cDNA pool derived from rosette leaf mRNAs of *Arabidopsis* using the primers PECT1/N-BamHI (see Supplemental Table 12 online) and PECT1/C-PstI (5'-AAACTGCAG-GAGTCTCCGGACACAAACGATTC-3'). The resulting PCR fragment was subcloned between the BamHI and PstI sites of the pQE30 expression vector (Qiagen), and the sequence was verified and designated pQE30-PECT1. *E. coli* expressing 6×His-PECT1 was suspended in a homogenizing buffer containing 50 mM Tris-HCl, pH 8.0, 10% (v/v) glycerol, 1 mM DTT, 10 mM ethylenediaminetetraacetic acid, and 1 mM phenylmethylsulfonyl fluoride. *E. coli* was then disrupted by a French pressure cell (135 MPa). After centrifugation, 6×His-PECT1 recovered in the pellet was solubilized in a buffer containing 20 mM phosphate buffer, pH 7.4, 500 mM NaCl, and 6 M urea. 6×His-PECT1 was then purified on a HisTrap column (Amersham Biosciences) according to the manufacturer's protocol. The recombinant protein was purified by SDS-PAGE before delivery to Sawady Technology.

The antiserum from Sawady Technology was purified on a HiTrap N-hydroxysuccinimide-activated high-performance column (Amersham Biosciences) conjugated with recombinant maltose binding protein-tagged PECT1 (MBP-PECT1) according to the manufacturer's protocol. To prepare MBP-PECT1, a PECT1 cDNA fragment from pQE30-PECT1 was subcloned into the BamHI and PstI sites of the pMal-c2X plasmid (New England Biolabs) and expressed in *E. coli* TB1. Cells were collected, suspended in a buffer containing 20 mM Tris-HCl, pH 8.0, 200 mM NaCl, 1 mM DTT, 1 mM EDTA, and 1 mM phenylmethylsulfonyl fluoride, and then disrupted by a French pressure cell as described above. After centrifugation at 9000g for 30 min at 4°C, the soluble fraction was purified on an amylose-affinity column (New England Biolabs) according to the manufacturer's protocol. Before applying the combined protein fractions onto the HiTrap N-hydroxysuccinimide-activated high-performance column, the protein buffer fractions were exchanged with one containing 0.2 M NaHCO₃, pH 8.3, and 0.5 M NaCl using a desalting column (PD-10; Amersham Biosciences).

Immunoblot Analysis

Immunoblot analysis of proteins extracted from *Arabidopsis* rosette leaves was conducted as described previously (Inatsugi et al., 2002).

Microscopy

Developing siliques were slit with a razor blade and then vacuum-infiltrated with ethanol:acetic acid (1:1, v/v) (Stangeland and Salehian, 2002) for observation with a differential interference contrast microscope equipped with Nomarski optics (BX50; Olympus). After incubation for 8 h, samples were transferred to a solution containing 74% (w/v) trichloroacetaldehyde monohydrate and 7.4% (v/v) glycerol for >1 d.

The following tissues were immersion-fixed in a mixture of 36% formaldehyde solution:acetic acid:70% ethanol (1:1:18, v/v) overnight at 4°C and then embedded in Technovit 7100 for sectioning (Heraeus Kulzer): (1) the fifth true leaves of 20-d-old plants that had just bolted; (2) mature stem samples taken from the bases of aged plants (i.e., 37 d old for wild-type plants and 47 d old for *pect1-4/pect1-6* F1 plants); and (3) roots of 6-d-old seedlings grown on agar medium. A microtome (RM2155; Leica Microsystems) was used to cut thin sections of 5 μm that were stained before bright-field observation (BX50; Olympus) with either (1) a 0.5% (w/v) toluidine blue solution in 0.1% Na₂CO₃ (w/v) or (2) 0.5% (w/v) hematoxylin in 5% ethanol, 1% (w/v) safranin O in aqueous solution (Waldeck), and 0.5% (w/v) fast green FCF in aqueous solution.

Seedlings or flowers were mounted on slides with water, as were stem samples from very young inflorescences after hand-sectioning with a razor blade. These tissues were observed with an epifluorescence microscope (BX50; Olympus). Three days after flowering, developing

seeds in the siliques of PECT1-EYFP plants were observed with a confocal laser-scanning microscope (TE2000-U with confocal system C1; Nikon) using an excitation beam at 488 nm and the emission filter HQ515/30m. To observe fluorescent proteins in root epidermis cells, PECT1-EYFP and 35S-EYFP seedlings were grown for 6 d on agar medium and then immersed for 30 min in a solution containing 500 nM MitoTracker Red CMXRos (Cambrex Bio Science), half-strength Murashige and Skoog salts, and 0.05% MES, pH 5.7. After a brief rinse in water, the roots were detached, mounted on slides, and examined for MitoTracker Red CMXRos fluorescence with a confocal laser-scanning microscope (excitation at 543 nm; emission filter HQ605LP/75m).

Lipid Extraction and Analysis

Lipids were extracted from whole rosettes or etiolated seedlings of *Arabidopsis* and quantified with a gas-liquid column chromatograph as described previously (Inatsugi et al., 2002).

Accession Numbers

Sequence data from this article can be found in the GenBank/EMBL data libraries under accession number At2g38670 (PECT1). Accession numbers for allelic *pect1* loci in the polymorphism database at The Arabidopsis Information Resource and those for PECT orthologs from other organisms in the GenBank/EMBL data libraries are listed in Table 1.

Supplemental Data

The following materials are available in the online version of this article.

Supplemental Table 1. Genetic Complementation of *pect1-6* Mutants.

Supplemental Table 2. Analysis of Embryos in the Developing Seeds of Self-Fertilized *PECT1/pect1-6* Siliques at 2 d after Flowering.

Supplemental Table 3. Analysis of Embryos in the Developing Seeds of Self-Fertilized *PECT1/pect1-6* Siliques at 4 d after Flowering.

Supplemental Table 4. Summary of Reciprocal Crosses of *PECT1/pect1-6* Plants.

Supplemental Table 5. Microscopic Analysis of Embryo Populations in Developing Seeds of Self-Fertilized *PECT1/pect1-4* Plants.

Supplemental Table 6. Microscopic Analysis of Embryo Populations in Developing Seeds of Self-Fertilized *PECT1/PECT1*, *PECT1/pect1-4*, and *pect1-4/pect1-4* Descendants of a *PECT1/pect1-4* Plant.

Supplemental Table 7. Analysis of Seeds within Self-Fertilized Siliques from Wild-Type and *pect1-4/pect1-6* F1 Plants.

Supplemental Table 8. Analysis of Seeds within Siliques from Manual Crosses between *PECT1/pect1-6* Female and *pect1-4/pect1-4* Male Plants.

Supplemental Table 9. Summary of Reciprocal Crosses between Wild-Type and *pect1-4/pect1-4* or *pect1-4/pect1-6* Plants.

Supplemental Table 10. Ovule Profiles in the Ovaries of Emasculated Flowers at 3 d after Emasculatation.

Supplemental Table 11. Fatty Acid Composition of Major Glycerolipids Found in Wild-Type, *pect1-4/pect1-4*, *pect1-4/pect1-6*, and *pect1-4/pect1-6 transPECT1* F1 Plants.

Supplemental Table 12. Determination of Genotype by CAPS, dCAPS, or PCR.

Supplemental Figure 1. Identification of Unusual Transcripts from the *pect1-6* Allele by RT-PCR.

Supplemental Figure 2. Glycerolipid Composition in Rosette Leaves and Etiolated Seedlings of Various *pect1* Plants.

ACKNOWLEDGMENTS

We thank Yoshibumi Komeda for helpful discussions and Munetaka Sugiyama for the use of a differential interference contrast microscope. We thank Pal Maliga for providing the pPZP211 and pPZP221 plasmids and Nam-Hai Chua for providing the pER8 plasmid. We also thank Koichiro Awai for discussion and critical reading of the manuscript. We appreciate the technical assistance of Atsuhiko Aoyama. This work was supported in part by the Program for the Promotion of Basic Research Activities for Innovative Biosciences and by a Grant-in-Aid for Priority Areas (17051004) from the Ministry of Education, Culture, Sports, Science, and Technology.

Received January 4, 2006; revised October 31, 2006; accepted November 10, 2006; published December 22, 2006.

REFERENCES

- Arabidopsis Genome Initiative** (2000). Analysis of the genome sequence of the flowering plant *Arabidopsis thaliana*. *Nature* **408**, 796–815.
- Babiychuk, E., Müller, F., Eubel, H., Braun, H.-P., Frentzen, M., and Kushnir, S.** (2003). *Arabidopsis* phosphatidylglycerophosphate synthase 1 is essential for chloroplast differentiation, but is dispensable for mitochondrial function. *Plant J.* **33**, 899–909.
- Baskin, T.I., and Bivens, N.J.** (1995). Stimulation of radial expansion in *Arabidopsis* roots by inhibitors of actomyosin and vesicle secretion but not by various inhibitors of metabolism. *Planta* **197**, 514–521.
- Beeckman, T., Przemek, G.K.H., Stamatou, G., Lau, R., Terry, N., De Rycke, R., Inzé, D., and Berleth, T.** (2002). Genetic complexity of cellulose synthase A gene function in *Arabidopsis* embryogenesis. *Plant Physiol.* **130**, 1883–1893.
- Birner, R., Bürgermeister, M., Schneiter, R., and Daum, G.** (2001). Roles of phosphatidylethanolamine and of its several biosynthetic pathways in *Saccharomyces cerevisiae*. *Mol. Biol. Cell* **12**, 997–1007.
- Bladergroen, B.A., and van Golde, L.M.G.** (1997). CTP:phosphoethanolamine cytidyltransferase. *Biochim. Biophys. Acta* **1348**, 91–99.
- Bogdanov, M., and Dowhan, W.** (1995). Phosphatidylethanolamine is required for *in vivo* function of the membrane-associated lactose permease of *Escherichia coli*. *J. Biol. Chem.* **270**, 732–739.
- Burk, D.H., Liu, B., Zhong, R., Morrison, W.H., and Ye, Z.-H.** (2001). A katanin-like protein regulates normal cell wall biosynthesis and cell elongation. *Plant Cell* **13**, 807–827.
- Clough, S.J., and Bent, A.F.** (1998). Floral dip: A simplified method for *Agrobacterium*-mediated transformation of *Arabidopsis thaliana*. *Plant J.* **16**, 735–743.
- Douce, R., Holtz, R.B., and Benson, A.A.** (1973). Isolation and properties of the envelope of spinach chloroplasts. *J. Biol. Chem.* **248**, 7215–7222.
- Emanuelsson, O., Nielsen, H., Brunak, S., and von Heijne, G.** (2000). Predicting subcellular localization of proteins based on their N-terminal amino acid sequence. *J. Mol. Biol.* **300**, 1005–1016.
- Emoto, K., and Umeda, M.** (2000). An essential role for membrane lipid in cytokinesis: Regulation of contractile ring disassembly by redistribution of phosphatidylethanolamine. *J. Cell Biol.* **149**, 1215–1224.
- Gamborg, O.L., Miller, R.A., and Ojima, K.** (1968). Nutrient requirements of suspension cultures of soybean root cells. *Exp. Cell Res.* **50**, 151–158.
- Hagio, M., Sakurai, I., Sato, S., Kato, T., Tabata, S., and Wada, H.** (2002). Phosphatidylglycerol is essential for the development of thylakoid membranes in *Arabidopsis thaliana*. *Plant Cell Physiol.* **43**, 1456–1464.
- Hajdukiewicz, P., Svab, Z., and Maliga, P.** (1994). The small, versatile pPZP family of *Agrobacterium* binary vectors for plant transformation. *Plant Mol. Biol.* **25**, 989–994.
- Heazlewood, J.L., Tonti-Filippini, J.S., Gout, A.M., Day, D.A., Whelan, J., and Millar, A.H.** (2004). Experimental analysis of the *Arabidopsis* mitochondrial proteome highlights signaling and regulatory components, provides assessment of targeting prediction programs, and indicates plant-specific mitochondrial proteins. *Plant Cell* **16**, 241–256.
- Hogetsu, T., Shibaoka, H., and Shimokoriyama, M.** (1974). Involvement of cellulose synthesis in action of gibberellin and kinetin on cell expansion. 2,6-Dichlorobenzonitrile as a new cellulose-synthesis inhibitor. *Plant Cell Physiol.* **15**, 389–393.
- Inatsugi, R., Nakamura, M., and Nishida, I.** (2002). Phosphatidylcholine biosynthesis at low temperature: Differential expression of CTP:phosphorylcholine cytidyltransferase isogenes in *Arabidopsis thaliana*. *Plant Cell Physiol.* **43**, 1342–1350.
- Kelly, A.A., Froehlich, J.E., and Dörmann, P.** (2003). Disruption of the two digalactosyldiacylglycerol synthase genes *DGD1* and *DGD2* in *Arabidopsis* reveals the existence of an additional enzyme of galactolipid synthesis. *Plant Cell* **15**, 2694–2706.
- Kim, H.U., and Huang, A.H.C.** (2004). Plastid lysophosphatidyl acyltransferase is essential for embryo development in *Arabidopsis*. *Plant Physiol.* **134**, 1206–1216.
- Kim, H.U., Li, Y., and Huang, A.H.C.** (2005). Ubiquitous and endoplasmic reticulum-located lysophosphatidyl acyltransferase, LPAT2, is essential for female but not male gametophyte development in *Arabidopsis*. *Plant Cell* **17**, 1073–1089.
- Kinney, A.J.** (1993). Phospholipid head groups. In *Lipid Metabolism in Plants*, T.S. Moore, ed (Boca Raton, FL: CRC Press), pp. 259–284.
- Kiyono, K., Miura, K., Kushima, Y., Hikiji, T., Fukushima, M., Shibuya, I., and Ohta, A.** (1987). Primary structure and product characterization of the *Saccharomyces cerevisiae CHO1* gene that encodes phosphatidylserine synthase. *J. Biochem. (Tokyo)* **102**, 1089–1100.
- Koehler, C.M.** (2004). New developments in mitochondrial assembly. *Annu. Rev. Cell Dev. Biol.* **20**, 309–335.
- Kuge, O., Nishijima, M., and Akamatsu, Y.** (1986). Phosphatidylserine biosynthesis in cultured Chinese hamster ovary cells. II. Isolation and characterization of phosphatidylserine auxotrophs. *J. Biol. Chem.* **261**, 5790–5794.
- Menon, A.K., and Stevens, V.L.** (1992). Phosphatidylethanolamine is the donor of the ethanolamine residue linking a glycosylphosphatidylinositol anchor to protein. *J. Biol. Chem.* **267**, 15277–15280.
- Mileykovskaya, E., Sun, Q., Margolin, W., and Dowhan, W.** (1998). Localization and function of early cell division proteins in filamentous *Escherichia coli* cells lacking phosphatidylethanolamine. *J. Bacteriol.* **180**, 4252–4257.
- Mizoi, J., Nakamura, M., and Nishida, I.** (2003). A study of the physiological function of phosphatidylethanolamine in *Arabidopsis*. In *Advanced Research on Plant Lipids*, N. Murata, M. Yamada, I. Nishida, H. Okuyama, J. Sekiya, and H. Wada, eds (Dordrecht, The Netherlands: Kluwer Academic Publishers), pp. 377–380.
- Murashige, T., and Skoog, F.** (1962). A revised medium for rapid growth and bioassay with tobacco tissue cultures. *Physiol. Plant.* **15**, 473–497.

- Neff, M.M., Neff, J.D., Chory, J., and Pepper, A.E.** (1998). dCAPS, a simple technique for the genetic analysis of single nucleotide polymorphisms: Experimental applications in *Arabidopsis thaliana* genetics. *Plant J.* **14**, 387–392.
- Nicol, F., His, I., Jauneau, A., Vernhettes, S., Canut, H., and Höfte, H.** (1998). A plasma membrane-bound putative endo-1,4- β -D-glucanase is required for normal wall assembly and cell elongation in *Arabidopsis*. *EMBO J.* **17**, 5563–5576.
- Opekarová, M., Robl, I., and Tanner, W.** (2002). Phosphatidyl ethanolamine is essential for targeting the arginine transporter Can1p to the plasma membrane of yeast. *Biochim. Biophys. Acta* **1564**, 9–13.
- Plavidis, P., Ramaswami, M., and Tanouye, M.A.** (1994). The *Drosophila easily shocked* gene: A mutation in a phospholipid synthetic pathway causes seizure, neuronal failure, and paralysis. *Cell* **79**, 23–33.
- Robl, I., Grassl, R., Tanner, W., and Opekarová, M.** (2001). Construction of phosphatidylethanolamine-less strain of *Saccharomyces cerevisiae*. Effect on amino acid transport. *Yeast* **18**, 251–260.
- Rontein, D., Wu, W.-I., Voelker, D.R., and Hanson, A.D.** (2003). Mitochondrial phosphatidylserine decarboxylase from higher plants. Functional complementation in yeast, localization in plants, and overexpression in *Arabidopsis*. *Plant Physiol.* **132**, 1678–1687.
- Saito, C., Morita, M.T., Kato, T., and Tasaka, M.** (2005). Amyloplasts and vacuolar membrane dynamics in the living graviperceptive cell of the *Arabidopsis* inflorescence stem. *Plant Cell* **17**, 548–558.
- Somerville, C., and Browse, J.** (1991). Plant lipids: Metabolism, mutants, and membranes. *Science* **252**, 80–87.
- Stangeland, B., and Salehian, Z.** (2002). An improved clearing method for GUS assay in *Arabidopsis* endosperm and seeds. *Plant Mol. Biol. Rep.* **20**, 107–114.
- Steenbergen, R., Nanowski, T.S., Beigneux, A., Kulinski, A., Young, S.G., and Vance, J.E.** (2005). Disruption of the phosphatidylserine decarboxylase gene in mice causes embryonic lethality and mitochondrial defects. *J. Biol. Chem.* **280**, 40032–40040.
- Tang, F., and Moore, T.S., Jr.** (1997). Enzymes of the primary phosphatidylethanolamine biosynthetic pathway in postgermination castor bean endosperm. Developmental profiles and partial purification of the mitochondrial CTP:ethanolaminephosphate cytidylyltransferase. *Plant Physiol.* **115**, 1589–1597.
- Till, B.J., et al.** (2003). Large-scale discovery of induced point mutations with high-throughput TILLING. *Genome Res.* **13**, 524–530.
- Tzafrir, I., Dickerman, A., Brazhnik, O., Nguyen, Q., McElver, J., Frye, C., Patton, D., and Meinke, D.** (2003). The *Arabidopsis* SeedGenes project. *Nucleic Acids Res.* **31**, 90–93.
- Tzafrir, I., Pena-Muralla, R., Dickerman, A., Berg, M., Rogers, R., Hutchens, S., Sweeney, T.C., McElver, J., Aux, G., Patton, D., and Meinke, D.** (2004). Identification of genes required for embryo development in *Arabidopsis*. *Plant Physiol.* **135**, 1206–1220.
- van Hellemond, J.J., Slot, J.W., Geelen, M.J.H., van Golde, L.M.G., and Vermeulen, P.S.** (1994). Ultrastructural localization of CTP:phosphoethanolamine cytidylyltransferase in rat liver. *J. Biol. Chem.* **269**, 15415–15418.
- Wallis, J.G., and Browse, J.** (2002). Mutants of *Arabidopsis* reveal many roles for membrane lipids. *Prog. Lipid Res.* **41**, 254–278.
- Wang, X., and Moore, T.S., Jr.** (1991). Phosphatidylethanolamine synthesis by castor bean endosperm. Intracellular distribution and characteristics of CTP:ethanolaminephosphate cytidylyltransferase. *J. Biol. Chem.* **266**, 19981–19987.
- Xu, C., Yu, B., Cornish, A.J., Froehlich, J.E., and Benning, C.** (2006). Phosphatidylglycerol biosynthesis in chloroplasts of *Arabidopsis* mutants deficient in acyl-ACP glycerol-3-phosphate acyltransferase. *Plant J.* **47**, 296–309.
- Yang, W., Mason, C.B., Pollock, S.V., Lavezzi, T., Moroney, J.V., and Moore, T.S.** (2004). Membrane lipid biosynthesis in *Chlamydomonas reinhardtii*: Expression and characterization of CTP:phosphoethanolamine cytidylyltransferase. *Biochem. J.* **382**, 51–57.
- Yu, B., Wakao, S., Fan, J., and Benning, C.** (2004). Loss of plastidic lysophosphatidic acid acyltransferase causes embryo-lethality in *Arabidopsis*. *Plant Cell Physiol.* **45**, 503–510.
- Yu, B., Xu, C., and Benning, C.** (2002). *Arabidopsis* disrupted in *SQD2* encoding sulfolipid synthase is impaired in phosphate-limited growth. *Proc. Natl. Acad. Sci. USA* **99**, 5732–5737.
- Zheng, Z., Xia, Q., Dauk, M., Shen, W., Selvaraj, G., and Zou, J.** (2003). *Arabidopsis AtGPAT1*, a member of the membrane-bound glycerol-3-phosphate acyltransferase gene family, is essential for tapetum differentiation and male fertility. *Plant Cell* **15**, 1872–1887.
- Zuo, J., Niu, Q.-W., and Chua, N.-H.** (2000). An estrogen receptor-based transactivator XVE mediates highly inducible gene expression in transgenic plants. *Plant J.* **24**, 265–273.